PRESTRESS LOSSES IN NSM-CFRP FLEXURALLY STRENGTHENED RC BEAMS

Inês COSTA[1]
PhD – Engineer
ISISE – University of Minho
Department of Civil Engineering, Campus de Azurém, 4800-058 Guimarães, Portugal
inescosta@civitest.com

Joaquim BARROS
Full Professor
ISISE – University of Minho
Department of Civil Engineering, Campus de Azurém, 4800-058 Guimarães, Portugal
barros@civil.uminho.pt

Abstract

The use of prestressed near surface mounted fibre reinforced polymers (NSM-FRP) has been long acknowledged to be a suitable approach to strengthen and retrofit existing reinforced concrete structures. The application of a certain amount of prestress to the FRP prior to its installation provides a number of benefits, mainly related to crack width and deflection requisites at serviceability limit state conditions. After transferring the prestress to a structural element, some of the existing cracks can be closed, decreasing the vulnerability of the element to corrosion and, a certain amount of deflection can be recovered due to the introduced negative curvature. However, these benefits can only be assured if the prestress is properly preserved over time. In this context, three series of reinforced concrete beams, in a total of 10 beams, were strengthened with a prestressed carbon FRP laminate (CFRP) and monitored for about 40 days. The data obtained from these tests is in this paper presented and analysed. The observed losses of strain in the CFRP laminate were found to be mainly located in the extremities of the bonded length, while in the central zone most of the initial strain was well-preserved over time. Additionally, the highest CFRP strain losses were observed in the first 6 to 12 days after prestress transfer, suggesting that the benefits of prestressed NSM-FRP will not be considerably lost over time.

Keywords: Prestressed CFRP, Near Surface Mounted, Prestress losses, Instantaneous losses, Long term losses.

[1] Corresponding Author. Tel: +351 253315199.
E-mail address: inescosta@civitest.com (Inês G. Costa).

1 Introduction

Over the years, the use of fibre reinforced polymers (FRP) for the strengthening of existing structures has been investigated and developed. In fact, FRP bars have already been employed in several structures in Europe, North America and Asia and Australia [1]. However, the use of these materials is not limited to the simple substitution of reinforcing steel by composite bars, but can also be used in repair, rehabilitation and retrofitting operations. Since FRP materials are a practical substitute for conventional reinforcing steel, several authors have also considered the possibility of using them to produce prestressed concrete elements. The use of prestressed FRPs is capable of taking advantage of the superior capacity of the concrete under compression to create a material that is robust both under tension and compression. However, likewise traditional prestress technology using steel bars, the FRPs can experience losses of strain over time and, therefore, this reduction needs to be quantified in order to introduce its effect in the structural design.

In the case of a prestressed NSM-FRP strengthening system, which is usually performed by bonding a prestressed FRP material with a suitable adhesive into a slit made on the concrete cover, besides the losses produced by concrete creep and steel relaxation, other phenomena may compromise the long term effectiveness of the prestress. Considering the common design practice, the relaxation of the prestressing material is typically one of the variables controlling the long term effectiveness of this technology. However, particularly in the case of carbon FRPs (CFRPs), the relaxation is recognized to be insignificant [2-3] and therefore, its contribution can be disregarded. On the other hand, since the prestress transference process from the NSM-FRP to the surrounding concrete relies on the efficacy of a structural adhesive and not on a cement-based grout, the creep of this interface needs to be evaluated. In fact, several authors have already indicated that the creep of the adhesive plays an important role on the long term behaviour of a composite system [3-5], and therefore its evaluation is crucial.

In this scope, some researchers have already reported the experimental behaviour observed in lap shear joints strengthened with externally bonded FRPs (EBR) under sustained stress [6-8], as well as on reinforced concrete beams strengthened with prestressed FRP sheets [3,9]. As a matter of fact, some efforts were already made to analytically predict the loss of prestress in RC elements strengthened with EBR CFRPs, namely by Wang et al. [10]. However, the results obtained using this strengthening system may not reflect the behaviour observed in prestressed FRP applied according to the Near Surface Mounted (NSM). Note that in this last strengthening technique, both surfaces of the FRP actively contribute to the stress transference process and peeling-off failure mechanisms are less likely to occur. Moreover, the adhesive used in NSM applications is typically stiffer than the one used in EBR, which may lead to lower strain losses over time.

In order to address the lack of research in the topic of prestressed NSM-FRP strengthening, this paper reports the prestress losses observed in three series of reinforced concrete beams strengthened with a single CFRP laminate up to four different levels of prestress. The prestressing process is described in detail and the observed losses over a conventional time-span are presented and analysed.

2 Geometry and material properties

To assess the prestress losses experienced by the prestressed NSM laminates after installation, two reinforced concrete beams of 150×300×2400 mm^3 were initially prepared. These beams, which compose Series I, were reinforced with 2 steel bars of 10 mm diameter both in the tension and compression faces. Closed loop vertical stirrups of 6 mm diameter spaced at 75 mm and 25 mm cover were also installed in order to avoid shear failure when this beams are tested up to failure (a type of test not covered in the present paper). One CFRP laminate of 1.4×20 mm^2 cross section was installed in each of the beams in a notch of about 5×25 mm^2 opened in the tensile face of the beam. The beams were planned to be executed with a C20/25 concrete strength class, ribbed surface steel bars of 500 MPa yield stress (A500 NR) and a CFRP laminate of 2000 MPa tensile strength and 150 GPa elastic modulus.

In a subsequent phase, two groups of four beams with dimensions of 150×300×4000 mm^3 were prepared. The first four beams (Series II) were reinforced with 2 steel bars of 10 mm diameter in the top and bottom faces and 6 mm closed loop stirrups were installed with 100 mm spacing and 30 mm concrete cover. The last four beams, which composed Series III, were reinforced similarly to the previous Series, but using 12 mm diameter bars for the longitudinal reinforcement and 8 mm diameter stirrups. In both of these series, the dimensions of the notch were increased to about 5×30 mm^2.

During the preparation process, samples of each of the intervening materials were collected for material characterization and the obtained results are presented in Tables 1 to 3.

3 Prestress application and monitoring system

One of the most crucial tasks of this work is the application of NSM-CFRP prestressed laminates on reinforced concrete elements. For this purpose, a prestress line was designed and installed in the Civil Engineering Laboratory at the University of Minho [11]. Due to the specificities of this prestress line, the reinforced concrete beams were flipped upside down, and the strengthening process was applied with the strengthened surface up (Figure 1). The prestress load was applied to the CFRP laminate at an average loading rate of 0.5 kN/min, while during prestress release, to avoid damage in the CFRP-adhesive-concrete interfaces, the release rate was decreased to 0.3 kN/min. A detailed description of the procedure adopted can be found elsewhere [15].

During the whole prestressing process of Series I beams, 9 strain gauges installed in the CFRP laminate were monitored, as depicted in Figure 2. After complete prestress transference, the loss of strain was measured in the CFRP laminate for a period of approximately 1000 h. In the case of Series II and III, the number of monitored strain gauges was reduced to 3, positioned as depicted in Figure 3.

One of the reinforced concrete beams of Series I was strengthened with a CFRP prestressed up to 20% of its ultimate nominal strain, while the remaining one was strengthened up to 30%. This means that, as the nominal ultimate strain of this material is 2000 / 150 = 13.333‰, a prestress level of 20% indicates a target strain of 0.2 ×13.333 = 2.667‰, while a prestress level of 30% requires the application of 0.3 ×13.333 = 4.000‰. With respect to the beams of Series II and III, each one was strengthened with a CFRP laminate prestressed up to 20%, 30%, 40% and 50% *i.e.*, using an initial strain level of 2.667‰, 4.000‰, 5.333‰ and 6.667‰, respectively. For future reference, these beams are herein labelled as Si_j%, where ‘i’ corresponds to the series number (1, 2 or 3) and ‘j’ to the prestress level (20, 30, 40 or 50).

During prestress application, the strain on the CFRP increased almost linearly with the applied load, as depicted in Figure 4 for the case of Series I specimens. The final average pre-strain applied to the beams was in general fairly close to the intended levels. After reaching the expected strain in each of the laminates, the hydraulic system was locked for about 3 days, which corresponds to the curing period of the adhesive. During that time period, undulant movements of the strain signal were registered by all the strain gauges. Note that, due to these fluctuations the strain readings on the CFRP laminates at time of unloading where different from the ones registered immediately after application.

4 Prestress losses

4.1 Instantaneous losses

Due to the prestress transference process, a decrease of strain is experienced along the bonded length. The highest strain losses are expected in the extremities of the CFRP laminate since at that zone the strain is expected to be null. That elevated strain loss gradually decreases towards mid-span where the strain decrease is no longer affected by the transference process but instead by the negative curvature in the beam induced by the prestressed CFRP.

Since, as previously revealed, the strains at time of prestress release were different from the ones at time of prestress application, a summary of the strains registered at the relevant time instants is given in Table 4 for the case of Series I beams. Temperature was found to be the cause of the strain readings fluctuations as it will be demonstrated in section 4.2. Since during loading/unloading the temperature is nearly constant, it was assumed that during the sustained stress period, the effective strains on the materials were constant. Therefore, the strain before load application is null by default, while the strain immediately after application is denoted by ε_p in Table 4. In the subsequent columns, the strain before prestress release, ε'_p, and after prestress release, ε_f, are also reported. For future reference, it is visible in Table 4 that, in the case of S1_20%, all the strain readings increased from prestress application to prestress release, as did the temperature. Inversely, the CFRP laminate in S1_30% experienced a decrease in installed strain similarly to the environmental temperature. According to the values reported in this table, it is remarkable that most CFRP strain gauges experienced relatively low strain losses, $\Delta\varepsilon_p / \varepsilon_p \times 100$, where $\Delta\varepsilon_p = \varepsilon_f - \varepsilon'_p$. In fact, the percentage of strain losses in the strain gauges positioned at a distance from the bond extremity higher than 125 mm was about 1% in S1_20% and 2% in S2_30%.

The same analysis of strains was performed for the case of the beams belonging to Series II and III and these results are reported in Tables 5 and 6. Similarly to the first two beams, the strain on the CFRP increased with the environmental temperature during the sustained load period.

The strain decrease profile during unloading is depicted in Figure 5 for the case of Series I beams. Note that to improve the interpretation of this graph, the strain recovery of the strain gauge placed outside the bonded length is not fully presented since it decreased to approximately zero when the applied load becomes null, as expectable. According to Figure 5, the most elevated strain losses are clearly located in the strain gauge installed at 25 mm, as already reported in Table 4. In the case of S1_30%, the strain gauge installed at 75 mm also displays a significant strain loss, although before release, this precise strain gauge already demonstrated a considerably lower strain reading (3.672‰ at 75 mm versus 3.802‰~3.892‰ in the remaining strain gauges). In any case, the load-strain profile of this strain gauge is fairly parallel to the one installed in a symmetrical position, 2025 mm.

The selection of the position of the strain gauges in Series I, depicted in Figure 2, was also governed by the purpose of validating the symmetry of the process of prestress application and release. If Figure 2 is analyzed, it is visible that both the strain gauge at 75 mm and at 2025 mm are both located 75 mm from the nearest unbonded section (2100 mm - 2025 mm = 75 mm). The same happens in the case of the strain gauges at 125 mm and 1975 mm. For that reason, the strain evolution during prestress release in those symmetric positions is depicted in Figure 6. Observing these pictures, it is clear that the strain loss at 125 mm and 1975 mm was in each beam practically the same. Regarding the relationship between the strains at 2025 mm and 75 mm, although they are relatively parallel to the previous curves (1975 mm versus 125 mm), a divergent tendency is observed between S1_20% and S1_30%. While in S1_20%, the higher strain loss is registered on the strain gauge placed at 2025 mm (passive end side), in S1_30% the largest strain loss is observed at 75 mm (active end side). This discrepancy is believed to be related with the difficulty of assuring a proper adhesive penetration in the groove. Therefore, if voids were formed within the groove, the effective bonded length which absorbs the prestress load transference may have been inaccurately provided in one, or both, of the CFRP extremities.

4.2 Long term losses

After the prestress load applied to the CFRP laminate has been transferred to the beams, all the strains were continuously monitored. Again, undulant movements of the strains were detected over time. To better demonstrate this behaviour, Figure 7 depicts the strain and temperature readings in the beams prestressed at 20%. Note that in the first 2.5 days after prestress release, the strain readings in S1_20% fluctuated significantly over time (Figure 7a) following the same trend of the environmental temperature profile, depicted in Figure 7b. However, regarding S2_20%, the strain level was virtually preserved over time, similarly to the environmental temperature. Therefore, as demonstrated in Figure 7c, the mid-span strain in S1_20% exhibited a nearly linear relationship with temperature while S2_20% appears to be uninfluenced by temperature during this period.

The raw data obtained *i.e.*, the original data prior to the removal of the environmental effects, is depicted in the left-hand side of Figures 8a and 8b. Observing, for example, the strain registered in S1_20% until about 6 days of age, it is visible that most of the strain gauges recovered nearly the totality of their initial strain, at time of prestress transfer, which is unrealistic. Moreover, if S1_30% is taken as example, the same observation can be made not only shortly after prestress transfer, but also after about 30 days, which is even less realistic. Based on the conclusions drawn from Figure 7 and the observation of these unrealistic strain recoveries, it was decided to assume that the mid-span strain was preserved over time, and the variation of this strain signal was used to remove the noise recorded in the remaining strain gauges. This noise removal strategy can be described by Eq. 0. The result produced by this noise removal strategy is depicted on the right-hand side of Figures 8a and 8b.

$$\varepsilon_{corrected}(t) = \varepsilon_{original}(t) - \left(\varepsilon_{1050mm}(t) - \varepsilon_{1050mm}(0)\right) \quad (0)$$

where $\varepsilon_{corrected}(t)$ is the corrected strain recorded at given position at a time instant t, $\varepsilon_{original}(t)$ is the original strain recorded at the same position and at the same time instant t, and $\varepsilon_{1050mm}(0)$ and $\varepsilon_{1050mm}(t)$ are the strains recorded in the strain gauge located at mid-span immediately after prestress release ($t = 0$) and at the time instant t, respectively. For the case of Series II and III beams, the subscript '1050 mm' does not apply and should be renamed as '1850 mm'. It should be noted that the use of this equation is limited to normal environmental temperature conditions, under which the adhesive properties and its bond performance to concrete can be assumed unchanged. If during the tests the environmental temperature approaches to the glass transition temperature of the adhesive, the degradation of this bonding agent, namely due to the increase in deformability and the loss of chemical interaction with the CFRP and concrete, can be significant. In this case the proposed equation is no longer applicable.

Analysing the strain evolution on the CFRP of S1_20% after performing the strain correction (right-hand side of Figure 8a), it is visible that the majority of the strain gauges did not experience significant losses over time. The sensor exhibiting higher strain loss is, as expected, the one installed at 25 mm from the loaded-end. In this section (25 mm), the installed strain became relatively stable after 6 days. Regarding the strain gauges at 75 mm from the un-bonded zone (75 mm and 2025 mm), both demonstrated almost the same strain loss over time, as already observed during the prestress transfer process. Given this observation, it is suggested that the transference length necessary to produce almost null strain loss in this CFRP strengthening system is between 75 mm and 125 mm.

In S1_30%, depicted on the right-hand side of Figure 8b, the same observations can be applied. The majority of the strain gauges registered minor strain losses, while at the strain gauge installed at 25 mm the loss was more expressive. Furthermore, the strain gauges at 75 mm and 2025 mm registered a significant decrease of strain over time. However, a discrepancy between these two curves is evident in this beam since, in fact, these have a strain shift of about 0.25‰ from each other. This observation confirms the suspicion that the strain gauges installed at 75 mm and 2025 mm may in fact represent non-symmetric positions, as already pointed out.

Regarding the experimental results of the prestressed beams of Series II and III, only the results after environmental correction are presented in Figures 9 and 10. In terms of curve profile, all results are fairly similar to the ones observed in Series I. However, it is worth mentioning that in S2_40%, depicted in Figure 9c, the strain loss in the strain gauges placed at 25 mm and 100 mm was noticeably high, especially when compared to the strain losses in S2_50%. Additionally, it is also noteworthy that the strain loss in the strain gauge placed at 100 mm in S3_50% (Figure 10d) was particularly large when compared to the strain loss at mid-span (1850 mm). However, a deeper analysis of Table 6 permits concluding that ε_p at mid-span was already abnormally large when compared to the other monitored sections, creating in this case a false impression of excessive strain loss.

To fairly compare the results obtained in these beams, the normalized strain in the CFRP laminate was computed, using as reference the applied strain, ε_p, reported in Tables 4 to 6. The result of the normalization of the strains of Series I beams is depicted in Figure 11 where the percentage of applied strain in S1_20% and S1_30% is reported side by side. The strain loss in the most central strain gauges (200 mm, 850 mm and 1050 mm) is notoriously low since 98%~99% of CFRP strain was retained in S1_20% over time, while in S1_30% that percentage was slightly lower and about 97%~98%. For the strain gauge at 25 mm from the unbonded zone this plot shows that after strain stabilization, S1_20% retained about 64% of the strain initially applied, while S1_30% was able of preserving about 69% of the initial value. Regarding the strain gauges installed at 75 mm from the unbonded zone, extraneous readings were obtained. If only the strain gauge at 2025 mm is analyzed in both beams, the normalized strain in both beams is nearly the same (93% in S1_20% and 92% in S1_30%). However, in the strain gauges placed at 75 mm, the strain loss in S1_20% was only about 6% while in S1_30% was almost 14%. These observations confirm that these strain discrepancies may in fact be related to a deficient filling of the groove at time of strengthening and, therefore, an inaccurate labeling of the monitored sections may have occurred.

The same analysis was performed with respect to the beams of Series II and III, as depicted in Figures 12 and 13. Comparing the strain profile of S2_20% and S2_50% (Figures 12a and 12b), it is visible that both strain gauges placed at 25 mm exhibited a similar percentage of strain loss. However, the strain gauge placed at 100 mm exhibited a larger percentage of loss in S2_20% than in S2_50%. On the other hand, as previously pointed out, S2_40% exhibited a strain loss at 100 mm considerably larger than all the other beams of this Series.

Concerning Series III beams, the normalized strain loss profile of S3_20% and S3_30% are practically the same, as suggested by the symmetry observed in Figure 13a. Moreover, S3_40% still appears to exhibit an abnormal percentage of strain loss in the strain gauges at 25 mm and 100 mm, even larger than S3_50%, which once more suggests that in fact, the positioning of the strain gauges may not correspond to their effective position.

Regarding the time necessary to attain a stabilized strain profile in these specimens, the beams of Series II and III required a longer period, in general up to 12 days. Even so, a great percentage of strain loss is also observed for about 6 days after prestress release.

5 Conclusions

In this paper, the procedure used to apply prestressed NSM-CFRP laminates in three series of reinforced concrete beams and the subsequent monitoring of the prestress losses along the CFRP laminate was described and analysed. The desired prestress levels were successfully applied in all of the beams. During the application and subsequent monitoring period, the variation of the environmental temperature was found to be a key parameter to properly assess the effective strain in the different materials/sections.

Concerning the instantaneous behaviour of the prestressed beams, all beams registered low levels of strain loss along the majority of the bonded length. The largest losses of prestress in the CFRP sections were registered in the strain gauges located at 25 mm from the unbonded zone, and were found to occur in the first 6 to 12 days after prestress release. Since negligible strain losses were observed in the CFRP sections located 200 mm from the unbonded zones in the first series of beams, it can be assumed that for prestress levels lower than 4‰, the required transfer length is lower than 125 mm. However, given the reduced number of strain gauges installed on the CFRP laminate, it was not possible to verify this assumption in the beams of Series II and III. Nevertheless, given the low strain loss registered at 100 mm in the beams prestressed up to 50%, it can be assumed that the transfer length will not be significantly higher than 100 mm. In any case, this estimation proves that this prestress application procedure was efficiently applied along most of the strengthening length.

6 Acknowledgments

The research carried out is part of the project PreLami (PTDC/ECM/114945/2009).The first Author acknowledges the support provided by FCT grant, SFRH/BD/61756/2009. The authors would also like to acknowledge S&P for providing the epoxy adhesive and FRP laminate and Unibetão, Pregaia and Casais for providing the reinforced concrete beams.

7 References

[1] ACI 440R-96 (1996). “State-of-the-Art Report on Fiber Reinforced Plastic (FRP) Reinforcement for Concrete Structures.” *American Concrete Institute* (ACI), 68 pp.

[2] Lopez-Anido, R. A. and Naik, T. R. (2000). “Emerging Materials for Civil Engineering Infrastructure - State of the Art.” *American Society of Civil Engineers*, Reston, Virginia, US.

[3] Wang, W.-W.; Dai, J.-G.; Harries, K. A. and Bao, Q.-H. (2012). “Prestress Losses and Flexural Behavior of Reinforced Concrete Beams Strengthened with Posttensioned CFRP Sheets.” *Journal of Composites for Construction*, ASCE, 16(2), 207-216.

[4] Nordin, H. and Täljsten, B. (2006). “Concrete Beams Strengthened with Prestressed Near Surface Mounted CFRP.” *Journal of Composites for Construction*, ASCE, 10(1), 60-68.

[5] Quantrill, R. J. and Hollaway, L. C. (1998). “The flexural rehabilitation of reinforced concrete beams by the use of prestressed advanced composite plates.” *Composites Science and Technology*, Elsevier, 58(8), 1259-1275.

[6] Choi, K.-K.; Meshgin, P.; Taha, M. M. R. (2007). “Shear creep of epoxy as the concrete-FRP interfaces.” *Composites Part B: Engineering*, Elsevier, 38(5-6), 772-780.

[7] Diab, H. and Wu, Z. (2007). “A linear viscoelastic model for interfacial long-term behavior of FRP–concrete interface.” *Composites Part B: Engineering*, Elsevier, 39(4), 722-730.

[8] Meaud, C.; Jurkiewiez, B. and Ferrier, E. (2011). “Investigation of creep effects in strengthened RC structures through double lap shear testing.” *Composites Part B: Engineering*, Elsevier, 42(3), 359-366.

[9] Wu, Z. and Diab, H. (2007). “A linear viscoelastic model for interfacial long-term behavior of FRP-concrete interface.” *Journal of Composites for Construction*, ASCE, 11(5), 477-486.

[10] Wang, W.W.; Dai, J.G.; Harries, K.A. and Zhang, L. (2014). “Prediction of prestress losses in RC beams externally strengthened with prestressed CFRP sheets/plates.” *Journal of Reinforced Plastics and Composites*, SAGE, 33(8), 699-713.

[11] Costa, I. G and Barros, J. A. O. (2012). “Design and development of a hydraulic-electro-mechanical system to apply pre-stressed CFRP laminates according to the NSM technique in laboratory conditions.” *Technical report no. 12-DEC/E-10*, University of Minho, Guimarães, Portugal, 59 pp.

[12] ISO 527-5 (1997). “Plastics - Determination of tensile properties – Part 5: Test conditions for unidirectional fibre-reinforced plastic composites.” *International Organization for Standardization*, 12 pp.

[13] E365 (1993). “Hardened Concrete - Determination of the modulus of elasticity of concrete in compression.” *National Laboratory for Civil Engineering Specification*, 2 pp (in Portuguese).

[14] NPEN10002-1 (1990). “Metallic materials - Tensile testing. Part 1: Method of test (at ambient temperature).” *European Committee for Standardization* (CEN), 34 pp. (in Portuguese)

[15] Costa, I. G. (2014). “Prestressed Carbon Fibre laminates applied according to Near Surface Mounted technique to increase the flexural resistance of Reinforced Concrete beams.” *PhD thesis*, University of Minho, Guimarães, Portugal.

LIST OF FIGURES

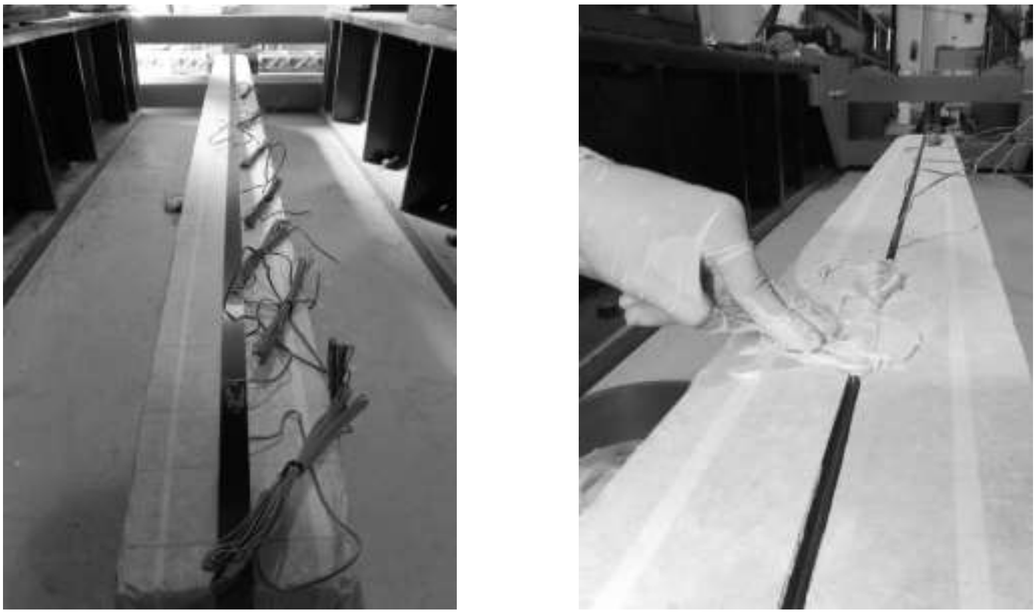

(a) (b)

Figure 1 – Prestress beam preparation: (a) installation of the strain gauges, (b) insertion of the adhesive.

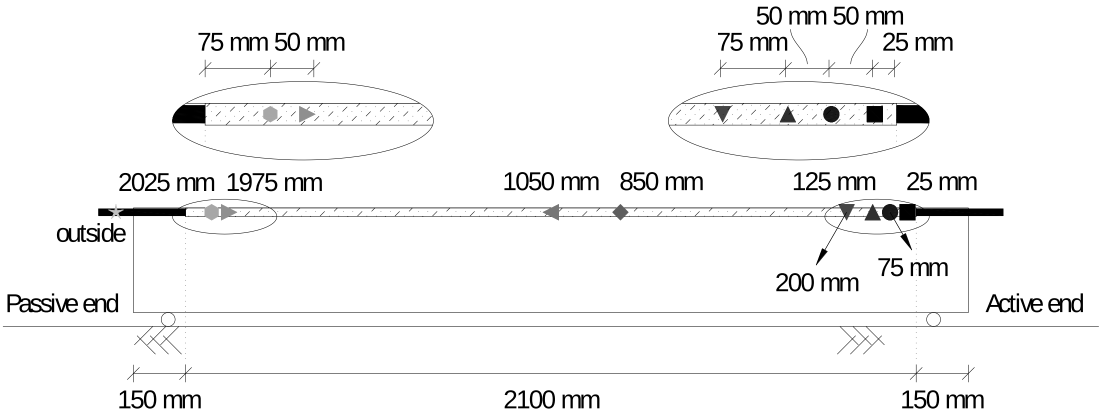

355 Figure 2 – Positioning of the strain gauges in the CFRP laminate – Series I.

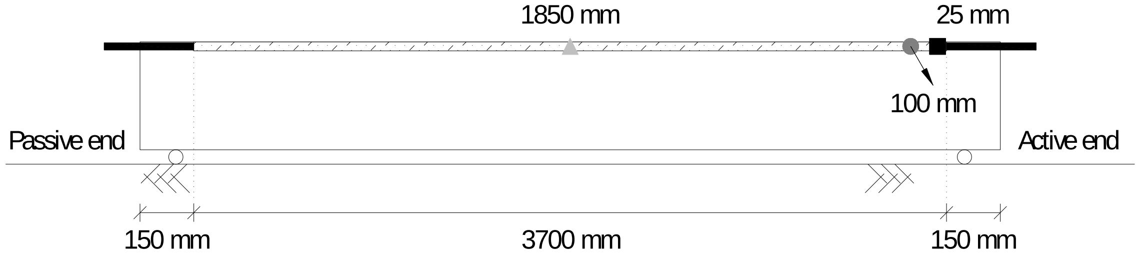

Figure 3 – Positioning of the strain gauges in the CFRP laminate – Series II and III.

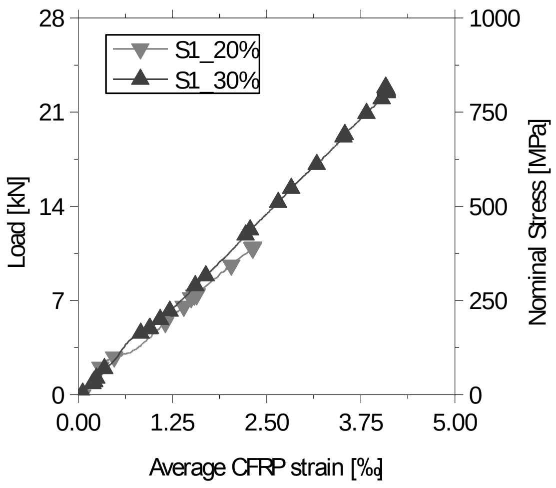

357 Figure 4 – Prestress load versus average CFRP strain during loading – Series I.

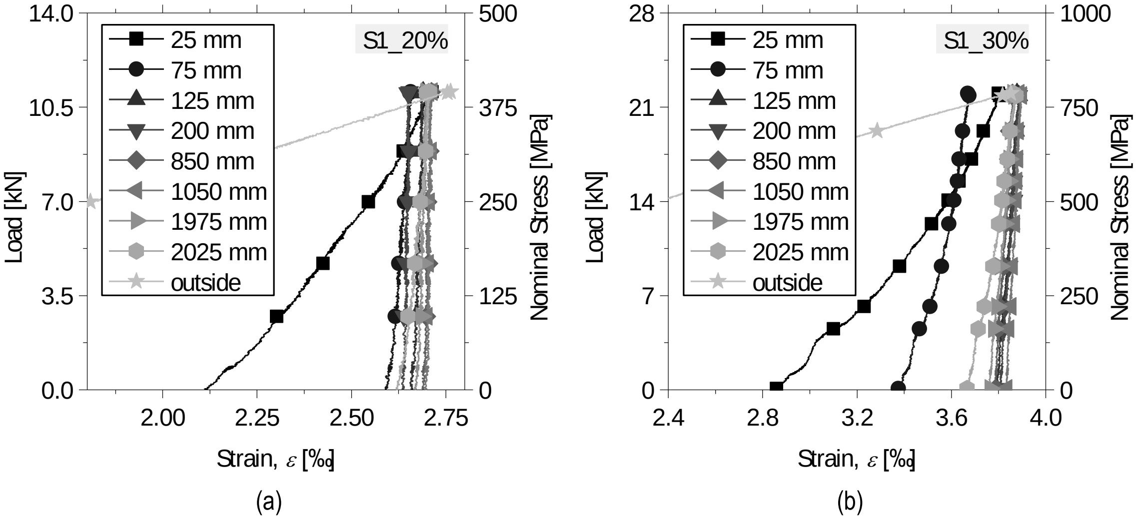

358 Figure 5 – Load versus strain in the CFRP during prestress release: (a) S1_20% and (b) S1_30%.

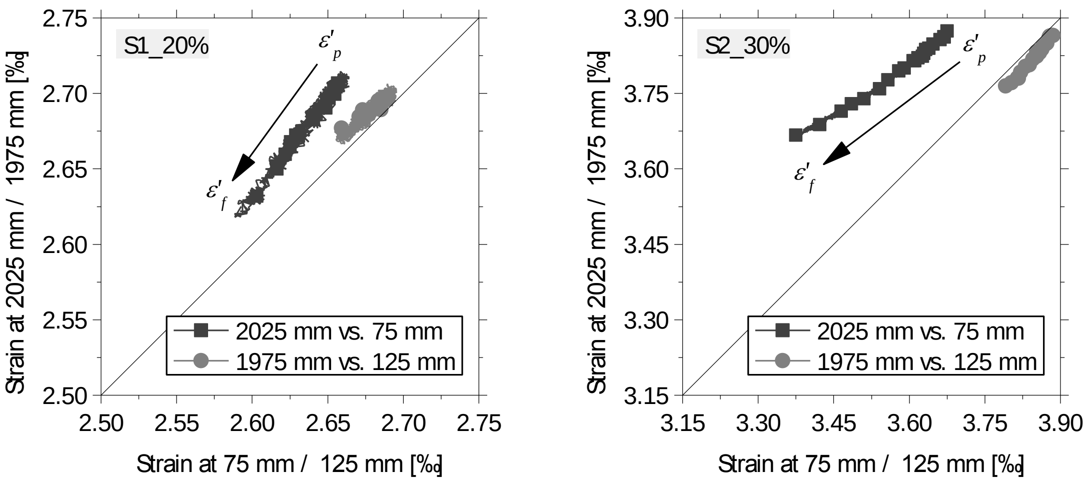

(a) (b)

Figure 6 – Strain evolution during prestress release in symmetrical CFRP strain gauges: (a) S1_20% and (b) S1_30%.

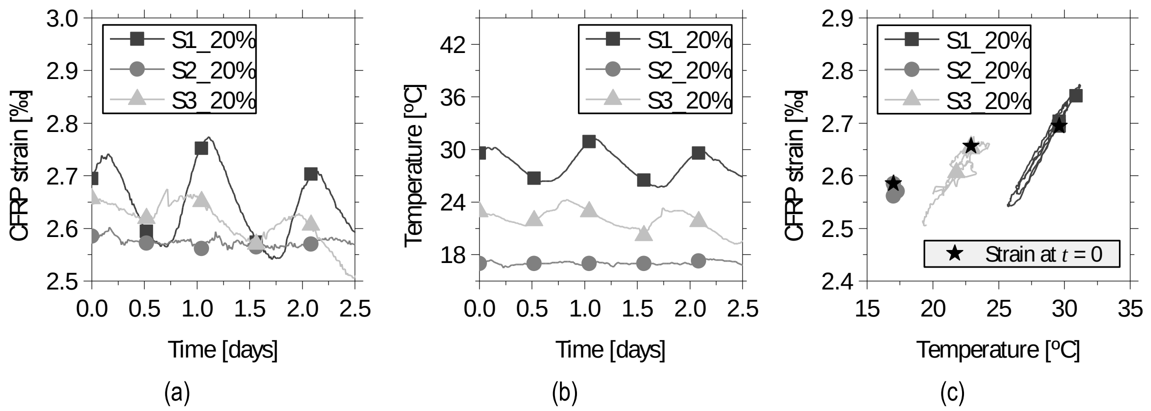

Figure 7 – Mid-span CFRP strains after prestress release: (a) strain versus time, (b) temperature versus time and (c) strain versus temperature.

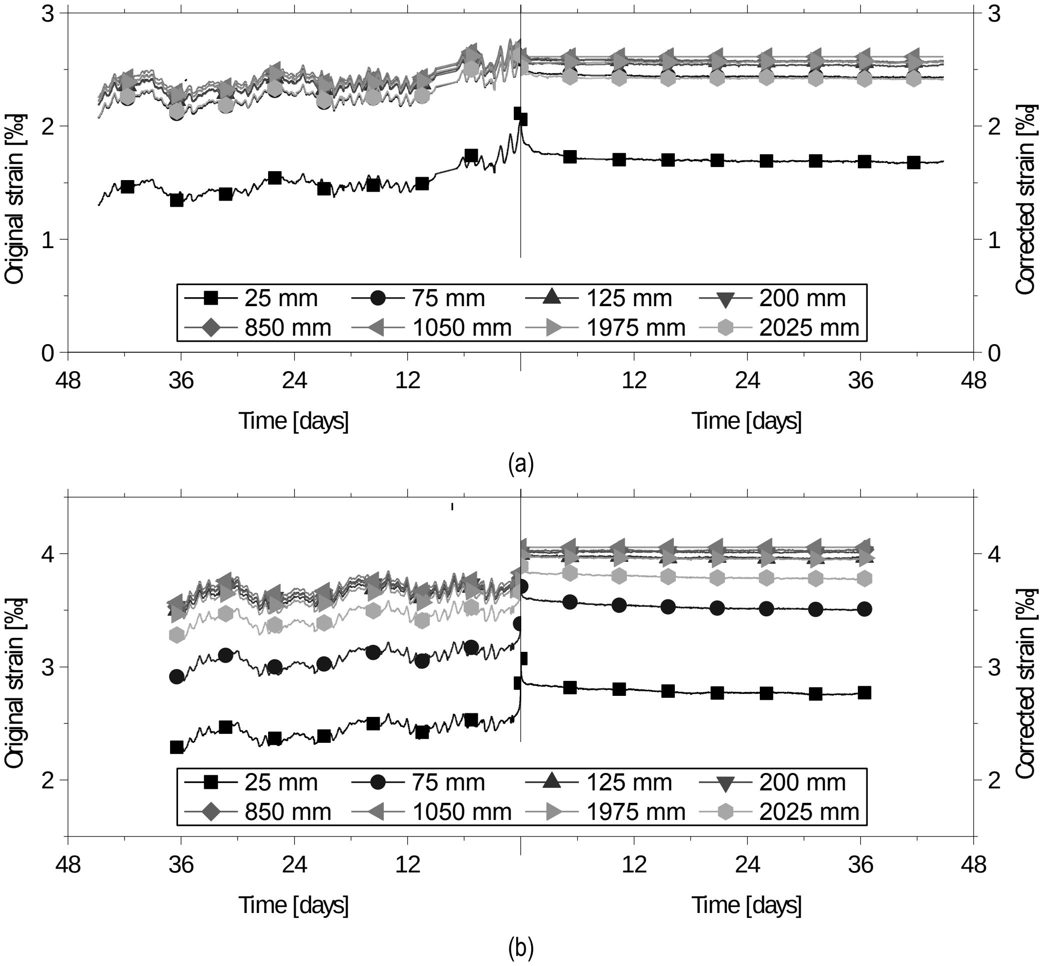

Figure 8 – Original and corrected CFRP strains: (a) S1_20% and (b) S1_30%.

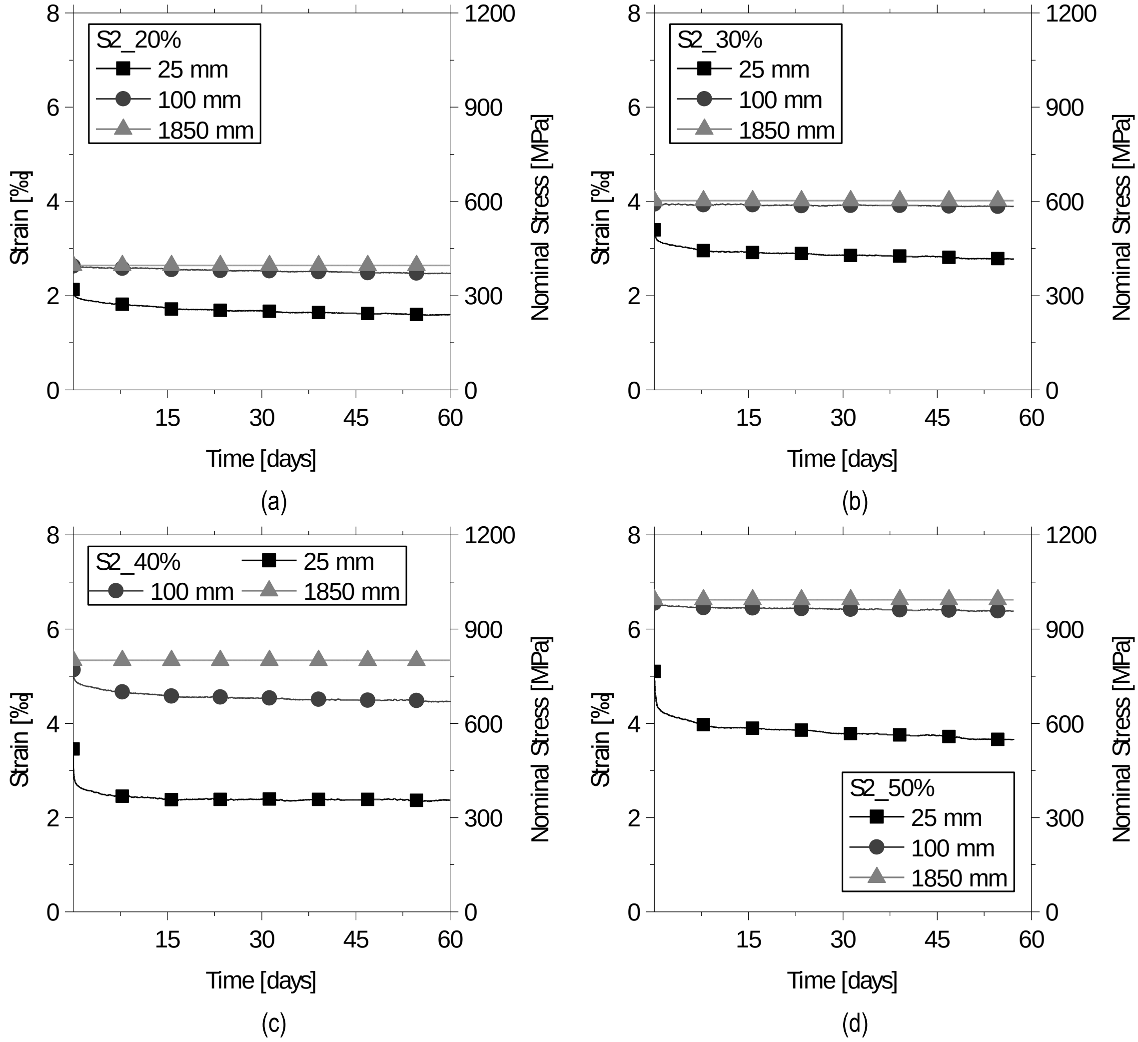

Figure 9 – Corrected CFRP strains: (a) S2_20%, (b) S2_30%, (c) S2_40% and (d) S2_50%.

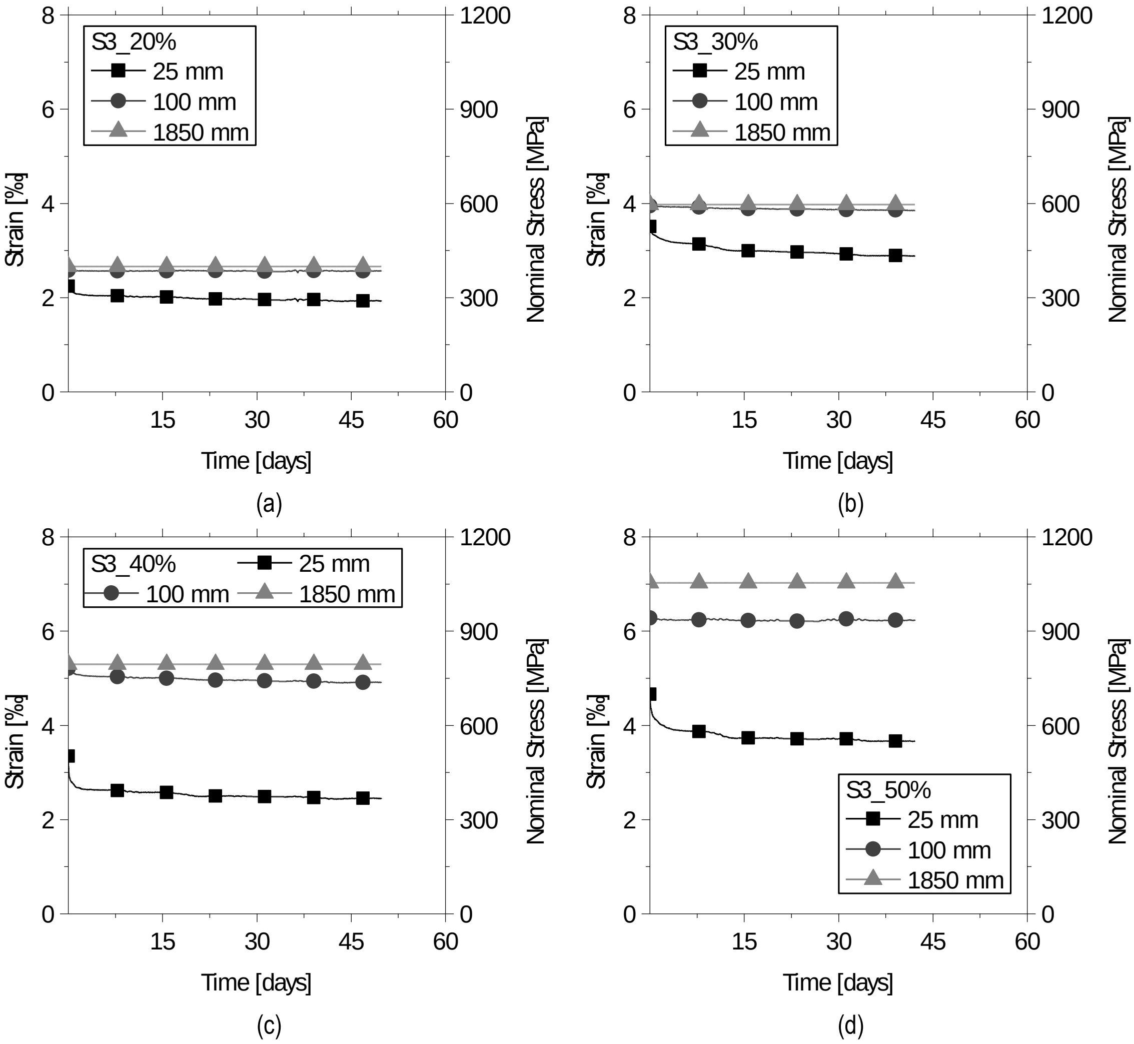

Figure 10 – Corrected CFRP strains: (a) S3_20%, (b) S3_30%, (c) S3_40% and (d) S3_50%.

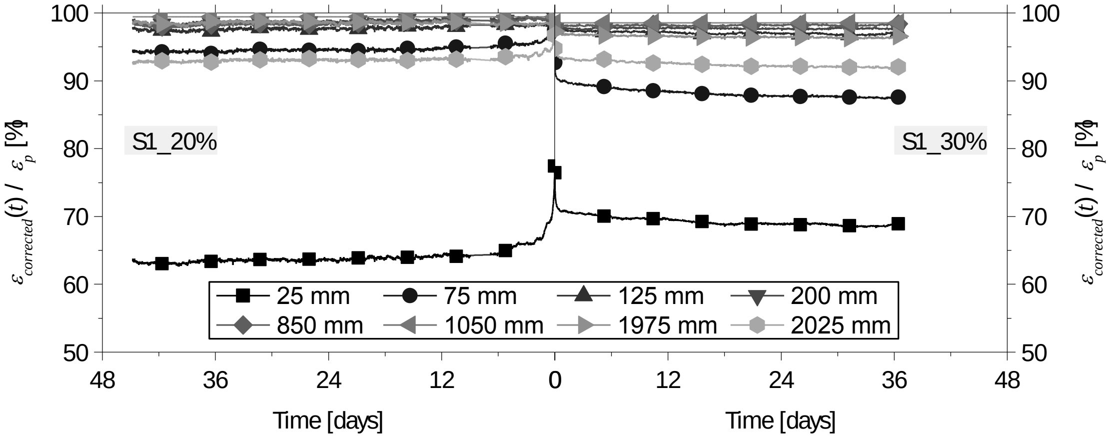

Figure 11 – Normalized strains over time in S1_20% (left) and S1_30% (right).

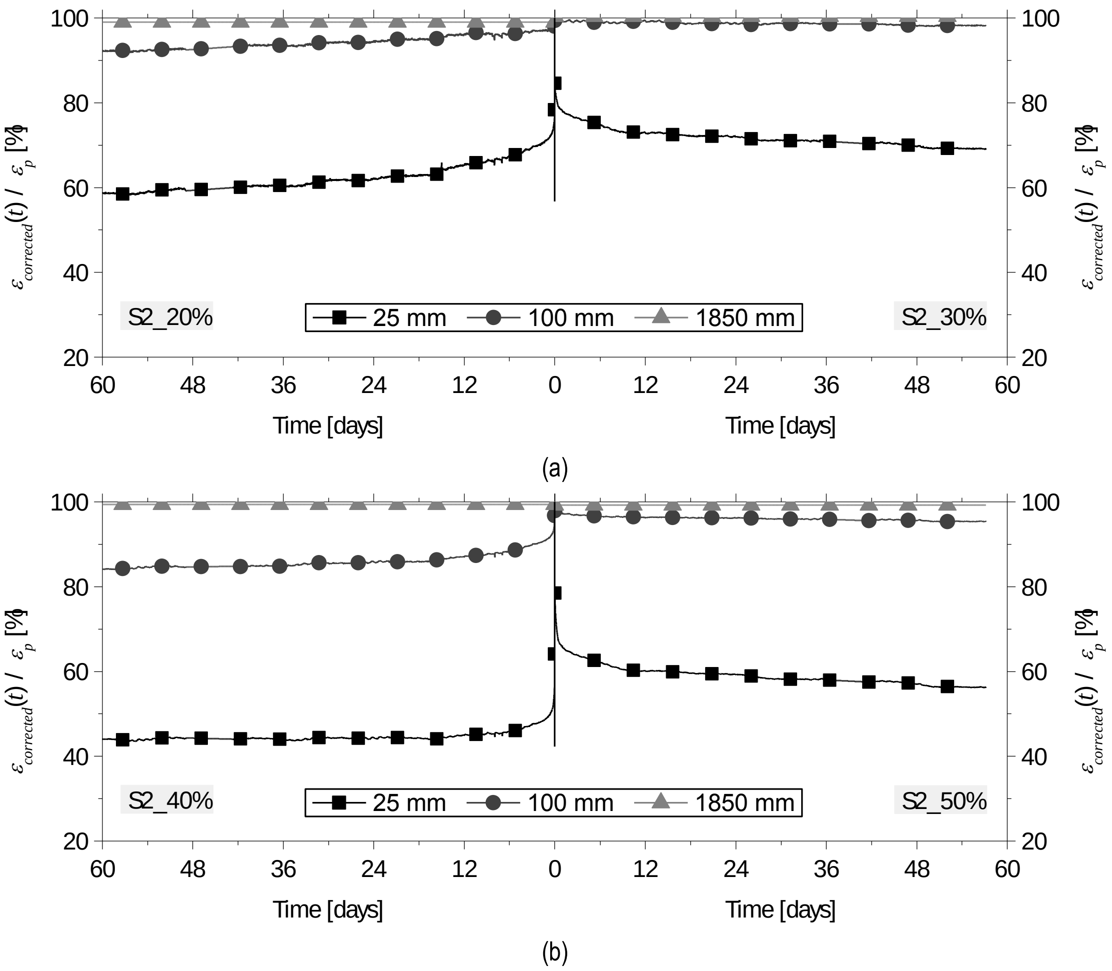

Figure 12 – Normalized strains over time in: (a) S2_20% (left) and S2_30% (right) and (b) S2_40% (left) and S2_50% (right).

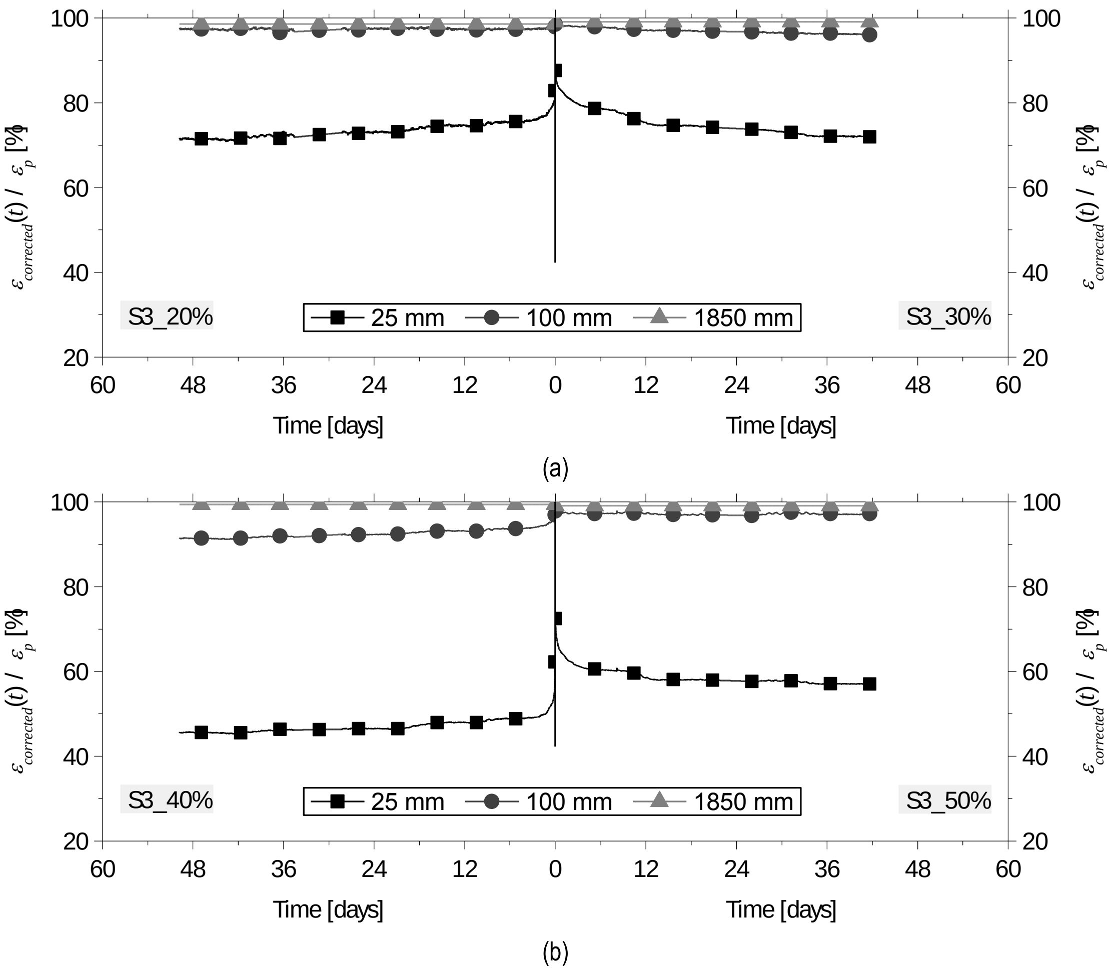

Figure 13 – Normalized strains over time in: (a) S3_20% (left) and S3_30% (right) and (b) S3_40% (left) and S3_50% (right).

List of Tables

Table 1 – Material properties – Series I [12-14].

Specimen	CFRP		Concrete		Reinforcing steel					
					Longitudinal bars			Stirrups		
	E_f [GPa]	f_f [MPa]	E_c [GPa]	f_c [MPa]	E_s [GPa]	f_y [MPa]	f_u [GPa]	E_s [GPa]	f_y [MPa]	f_u [GPa]
1	167	1925	29.10	33.0	203	515	635	218	629	703
2	167	1970	25.74	31.4	200	514	635	215	605	694
3	170	1859	- §	- §	210	519	640	228	618	703
4	170	1970	- §	- §	211	519	640	209	598	684
5	170	1941	-	-	216	513	632	-	-	-
Average	169	1933	27.4	32.2	208	516	636	218	613	696
Standard Deviation	2	46	2.4	1.1	6	3	4	8	14	9
COV	1%	2%	9%	3%	3%	1%	1%	4%	2%	1%

§ Some of the samples casted were mistakenly used for other purposes.

Table 2 – Material properties – Series II [13-14].

Specimen	Concrete		Reinforcing steel					
			Longitudinal bars			Stirrups		
	E_c [GPa]	f_c [MPa]	E_s [GPa]	f_y [MPa]	f_u [GPa]	E_s [GPa]	f_y [MPa]	f_u [GPa]
1	-	33.5 §	197	530	643	216	646	680
2	43.3	50.5	204	555	644	213	645	676
3	38.1	42.8	201	521	625	208	642	673
4	39.2	50.1	212	541	630	216	653	685
5			202	544	632	204	653	688
Average	40.2	47.8	202	538	634	211	648	680
Standard Deviation	2.8	4.3	6	12	8	5	5	6
COV	7%	9%	3%	2%	1%	3%	1%	1%

§ Considered as an outlier and, therefore, not considered in the average calculation.

Table 3 – Material properties – Series III [13-14].

Specimen	Concrete		Reinforcing steel					
			Longitudinal bars			Stirrups		
	E_c [GPa]	f_c [MPa]	E_s [GPa]	f_y [MPa]	f_u [GPa]	E_s [GPa]	f_y [MPa]	f_u [GPa]
1	-	31.4	181	518	626	194	535	641
2	38.54	36.0	213	527	625	196	547	645
3	39.27	31.2	206	517	622	200	541	646
4	41.38	27.8	218	517	624	-	-	-
5	-	-	201	521	621	-	-	-
Average	39.7	31.6	204	520	624	197	541	644
Standard Deviation	1.5	3.4	14	4	2	3	6	3
COV	4%	11%	7%	1%	0%	1%	1%	0%

Table 4 – Instantaneous prestress losses – Series I.

Strain gauge	S1_20%					S1_30%				
	ε_p [‰]	ε'_p [‰]	ε_f [‰]	$\Delta\varepsilon_p$ [‰]	$Loss$ [%]	ε_p [‰]	ε'_p [‰]	ε_f [‰]	$\Delta\varepsilon_p$ [‰]	$Loss$ [%]
25 mm	2.657	2.710	2.110	0.600	23	4.020	3.802	2.855	0.947	24
75 mm	2.579	2.658	2.594	0.065	3	4.005	3.672	3.378	0.294	7
125 mm	2.632	2.691	2.658	0.032	1	4.089	3.886	3.791	0.094	2
200 mm	2.573	2.655	2.640	0.015	1	4.107	3.892	3.798	0.094	2
850 mm	2.619	2.710	2.690	0.021	1	4.103	3.864	3.784	0.080	2
1050 mm	2.627	2.709	2.695	0.015	1	4.116	3.891	3.832	0.059	1
1975 mm	2.603	2.698	2.668	0.029	1	4.101	3.871	3.759	0.112	3
2025 mm	2.603	2.712	2.626	0.085	3	4.107	3.874	3.659	0.215	5
outside	2.602	2.767	0.152	2.615	100	4.100	3.858	-0.017	3.875	95
Temperature [ºC]	19.5	29.7				29.4	17.7			

$\Delta\varepsilon_p = \varepsilon_f - \varepsilon'_p$; $Loss = \Delta\varepsilon_p / \varepsilon_p \times 100$

Table 5 – Instantaneous prestress losses – Series II.

	S2_20%					S2_30%				
Strain gauge	ε_p	ε'_p	ε_f	$\Delta\varepsilon_p$	$Loss$	ε_p	ε'_p	ε_f	$\Delta\varepsilon_p$	$Loss$
	[‰]	[‰]	[‰]	[‰]	[%]	[‰]	[‰]	[‰]	[‰]	[%]
25 mm	2.718	2.662	2.072	0.590	22	4.018	3.953	3.326	0.627	16
100 mm	2.684	2.628	2.575	0.053	2	3.968	3.897	3.871	0.027	1
1850 mm	2.667	2.612	2.585	0.026	1	4.000	3.912	3.923	-0.012	0
Temperature [ºC]	15.7	16.7				16.9	17.4			
	S2_40%					S2_50%				
Strain	ε_p	ε'_p	ε_f	$\Delta\varepsilon_p$	$Loss$	ε_p	ε'_p	ε_f	$\Delta\varepsilon_p$	$Loss$
	[‰]	[‰]	[‰]	[‰]	[%]	[‰]	[‰]	[‰]	[‰]	[%]
25 mm	5.388	5.291	3.355	1.935	36	6.499	6.475	5.075	1.400	22
100 mm	5.304	5.177	5.006	0.171	3	6.693	6.648	6.509	0.139	2
1850 mm	5.370	5.317	5.285	0.032	1	6.672	6.622	6.572	0.050	1
Temperature [ºC]	15.7	16.7				16.9	17.4			

$\Delta\varepsilon_p = \varepsilon_f - \varepsilon'_p$; $Loss = \Delta\varepsilon_p / \varepsilon_p \times 100$

Table 6 – Instantaneous prestress losses – Series III.

	S3_20%					S3_30%				
Strain gauge	ε_p	ε'_p	ε_f	$\Delta\varepsilon_p$	$Loss$	ε_p	ε'_p	ε_f	$\Delta\varepsilon_p$	$Loss$
	[‰]	[‰]	[‰]	[‰]	[%]	[‰]	[‰]	[‰]	[‰]	[%]
25 mm	2.704	2.740	2.281	0.459	17	4.009	3.721	3.224	0.497	12
100 mm	2.637	2.635	2.585	0.050	2	4.009	3.739	3.677	0.062	2
1850 mm	2.700	2.698	2.656	0.041	2	4.014	3.702	3.666	0.035	1
Temperature [ºC]	20.6	23.3				23.1	18.4			
	S3_40%					S3_50%				
Strain	ε_p	ε'_p	ε_f	$\Delta\varepsilon_p$	$Loss$	ε_p	ε'_p	ε_f	$\Delta\varepsilon_p$	$Loss$
	[‰]	[‰]	[‰]	[‰]	[%]	[‰]	[‰]	[‰]	[‰]	[%]
25 mm	5.373	5.362	3.313	2.049	38	6.425	6.018	4.250	1.768	28
100 mm	5.376	5.401	5.206	0.195	4	6.416	6.047	5.908	0.139	2
1850 mm	5.329	5.327	5.265	0.062	1	7.087	6.453	6.391	0.062	1
Temperature [ºC]	20.6	23.3				23.1	18.4			

$\Delta\varepsilon_p = \varepsilon_f - \varepsilon'_p$; $Loss = \Delta\varepsilon_p / \varepsilon_p \times 100$